

# Local analysis of wave fields from hindcasted sea states for rogue wave risk evaluations

F. Dias, J. Brennan, J. M. Dudley, C. Viotti  
funded by the ERC AdG MULTIWAVE  
2012-2016

August 5, 2014

---

## OPTICAL TURBULENCE

A. C. NEWELL

Arizona Center for the Mathematical Sciences,  
Tucson, AZ 85721, USA

V. E. ZAKHAROV

Landau Institute for Theoretical Physics,  
Chernogolovka, Russia

---

This essay is a “c'mon over” invitation to the battered veterans of the war to tame the turbulence realized by the whimsical and capricious solutions of the high Reynolds number limit of the Navier-Stokes equations. **Simple fluids are easier to drink than understand.** They admit no nontrivial limiting behaviors, no convenient footholds from which the theoretician can launch his first assault. When the flow is interesting, every term in the

jects are robust (the events are not rare and each event, once begun, is very stable) and almost singular solutions of the Navier-Stokes equations. They appear at random points at space and time, and are usually short lived. They, too, play a role in determining transport properties and dissipation rates. In particular, they contribute to the intermittency of turbulence, the bursts of large fluctuations that affect the tails of the joint probability density



*“Simple fluids are easier to drink than understand.”*

--**A.C. Newell** and **V. E. Zakharov**, in Turbulence: A Tentative Dictionary ( Plenum Press, NY 1994)



Corollary:

*“Simple fluids are easier to understand if you drink.”*



From Niemela



# The Extreme Waves Map of Ireland

Ireland is battered by waves from all sides and has suffered many extreme oceanic events. From one of the largest known underwater landslides in the world at Storegga to the tragedy of the Fastnet Yacht race; from tsunamis in Kinsale to the navy vessel *Róisín* battered by rogue waves, it is clear that Ireland has experienced a wide variety of ocean extremes. This map presents the first catalogue of such events, dating as far back as the turn of the last ice age. Detailed studies of this kind are important both to understand the science of the ocean wave environment of Ireland, and also for applications such as improving the safety of shipping and coastal structures, and generating renewable energy from the sea. They can also provide new insights into myths and legends, and the origin of many unexplained features of our natural environment.

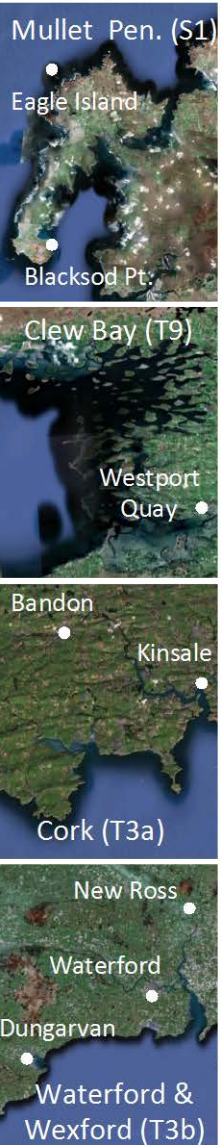


## Legend

- ### Storm Waves
- S1 1837, 1861, 1894, 1935, 1987, 1988 and 1989  
The Mullet Peninsula, Co. Mayo
  - S2 1869 and 1881: Calf Rock, Co. Cork
  - S4 1864: Valentia, Co. Kerry
  - S5 1877: Railway Lines, Co. Dublin and Co. Wicklow
  - S6 1899: Greenore, Carlingford Lough, Co. Louth
  - S7 1941: Inisheer Lighthouse, the Aran Islands
  - S8 1945: Rosslare, Co. Wexford
  - S9 1951: Kilkee, Co. Clare
  - S10 1953: the Aran Islands
  - S11 1962: Co. Cork
  - S12 1974: Kilmore, Co. Wexford
  - S13 1979: Fastnet Race
  - S14 1982: Ventry, Co. Kerry
  - S15 1985: Fastnet Rock Lighthouse

- ### Tsunamis
- T1 14,680 BP: the Barra Fan, Peach Slide
  - T2 8200 BP: Storegga slide
  - T3 1755, 1761, 1941 and 1975:  
The Lisbon, Portugal tsunamis
  - T4 1767: The River Liffey, Dublin
  - T5 1841: Kilmore, Co. Wexford
  - T6 1854: Kilmore, Co. Wexford
  - T7 1894: Galway Bay and The Atlantic  
(*Festina Lente* and *Manhattan*)
  - T8 1922: Ballycotton, Co. Cork
  - T9 1909: Westport Quay, Co. Mayo
  - T10 1910: Cork, Waterford, Southampton, Jersey, Dublin and Ilfracombe
  - T11 1912: Bray, Co. Wicklow
  - T12 1932: Inishowen, Co. Donegal

- ### Rogue Waves
- R1 1852: Inis Mór, The Aran Islands
  - R2 1883: Youghal, Co. Cork
  - R3 1899: Kilkee, Co. Clare
  - R4 1914: Iniskeeragh, off Donegal
  - R5 1936: Dundalk, Co. Louth
  - R6 1972: Mullaghderg, Donegal
  - R7 2004: L.E. *Róisín*, off Donegal coast
  - R8 2006: off Portrush, Co. Antrim
  - R9 2006: Ardglass, Co. Down
  - R10 2007: Doonbeg, Co. Clare
  - R11 2007: Valentia Island, Co. Kerry
  - R12 2011: Swanland, off Bardsey Island, Irish Sea
  - R13 2011: Largest wave recorded in Ireland



Extreme wave events in Ireland: 14680 BP–2012  
L. O'Brien, J. M. Dudley and F. Dias. *Nat. Hazards Earth Syst. Sci.*, **13**, 1–24, 2013

© Map Layout copyright L. O'Brien, J. M. Dudley, F. Dias

# The Extreme Waves Map of Ireland

[Irish Newspaper Archives](#)

Irish Press 1931-1995, 10.03.1962, page 5

1962!

## **FREAK WAVE**

The Spanish fishing vessel Maria Domenguez arrived at Bantry pier yesterday with the entire front structure of the wheelhouse torn from its foundation.

# 2013 – 2014 WINTER IN IRELAND



Loop Head,  
Ireland

This cliff is about  
30 m high

01 February 2014

Princeton 17 July 2014

# Introduction

- Rogue waves have been the topic of many intense studies over the last couple of years, with much ground covered theoretically, experimentally, and numerically, providing an understanding of the physics of rogue waves.
- There have also been several rogue wave events recorded in the open ocean, such as the Draupner and Andrea events, and unfortunately some maritime disasters associated with these freak events.
- Global scale wave climate models such as Wavewatch III and WAM are capable of hindcasting such events, providing accurate sea state descriptions from which various wave field parameters can be obtained, such as significant wave height, mean wave direction, etc

- However, such hindcasts are limited to 2 dimensional wave fields which are coarse grained, and unable to reproduce the instantaneous surface position at a given time.
- On the other hand, local wave models based on first principle fluid dynamics provide high resolution time evolution of the water surface elevation, from which refined wave statistics can be obtained.
- These models, in general, are difficult to interface with the full complexity of real world sea conditions
- Presented here are our preliminary efforts along this route. Taking hindcasted field data from the Andrea event as an initial condition, we simulate 3D random wave fields using a higher order spectral method.



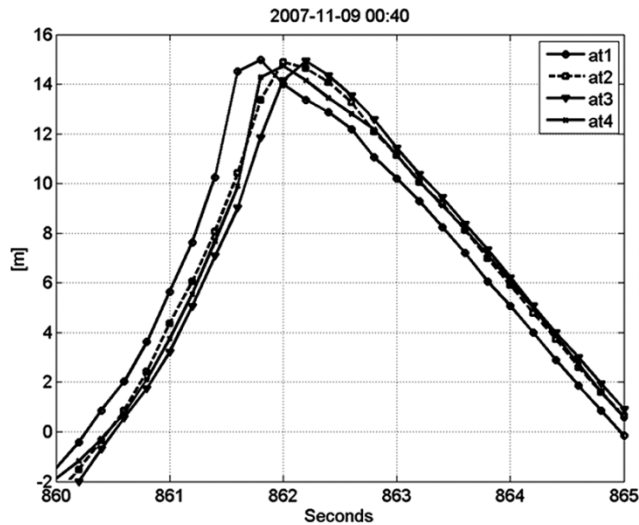
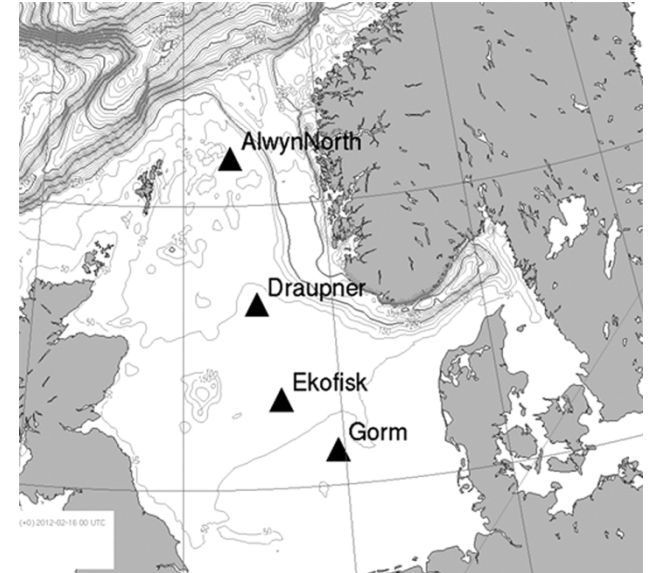
# Andrea Wave

The Andrea Wave was at the Ekofisk platform complex in the North Sea, during the so called Andrea Storm passing through the area at the time. A quick summary of some of the important facts of the storm:

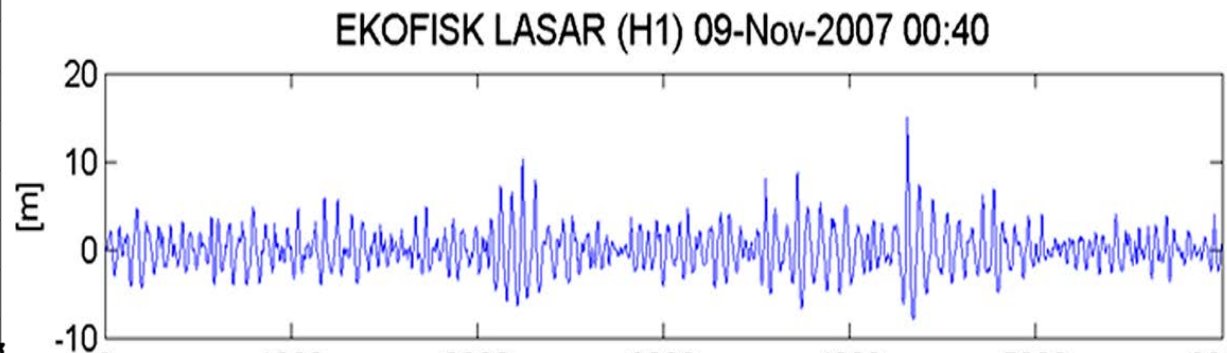
- crossed the North Sea on 8<sup>th</sup> – 9<sup>th</sup> November 2007
- it followed a low pressure area, moving from southern Norway to southern Sweden, along with strong westerly winds (50-55 knots)
- On the 8<sup>th</sup>, a high wave field was built up around the north area of the Ekofisk platform, with wave heights of 10-11 m recorded in the evening
- On the 9<sup>th</sup>, the wind field passed through the north and north-east Ekofisk field, with wave heights of 11-12 m being recorded.

# A NEW WELL DOCUMENTED ROGUE WAVE : THE ANDREA WAVE

Wave profiles have been measured with a system of 4 lasers mounted on a bridge at the oil production site Ekofisk in the central North Sea since 2003. A rogue wave was measured on Nov. 9, 2007 in a storm crossing the North Sea and named Andrea – Magnusson & Donelan (2013) "*The Andrea Wave Characteristics of a Measured North Sea Rogue Wave*"



*Time in seconds*



Wave profile time series during 20 min with 5 Hz sampling frequency

Princeton 17 July 2014

The Andrea wave itself occurred just passed 00:00 UTC on the 9<sup>th</sup>, by down looking Optech lasers on site at the Ekofisk platform.  
Some wave characteristics from the event:

$$H_s = 9.2m$$

$$T_p = 13.2s$$

$$H_{max} = 21.1m$$

$$CH_{max} = 15.0m$$

$$H_{max}/H_s = 2.3$$

$$CH_{max}/H_s = 1.63$$

Rogue wave classification:

$$CH_{max} > 1.25H_s \quad H_{max} > 2H_s \quad (1)$$

# Andrea Wave

## Hindcast Data

- Hindcast data obtained from the ECMWF data archive is used as initial condition for the local scale HOSM model.
- The covered time period is 00:00 UTC 8<sup>th</sup> - 00:00 UTC 10<sup>th</sup> November 2007, stored at 6 hour intervals
- The data contains the directional wave spectrum, corresponding to the closest grid point to the Ekofisk platform.
- The spectrum at 00:00 UTC on the 9<sup>th</sup>, the closest time point to the Andrea event, is extracted for analysis.
- The directional wave spectrum must be converted to a wavenumber spectrum to be used as an initial condition.



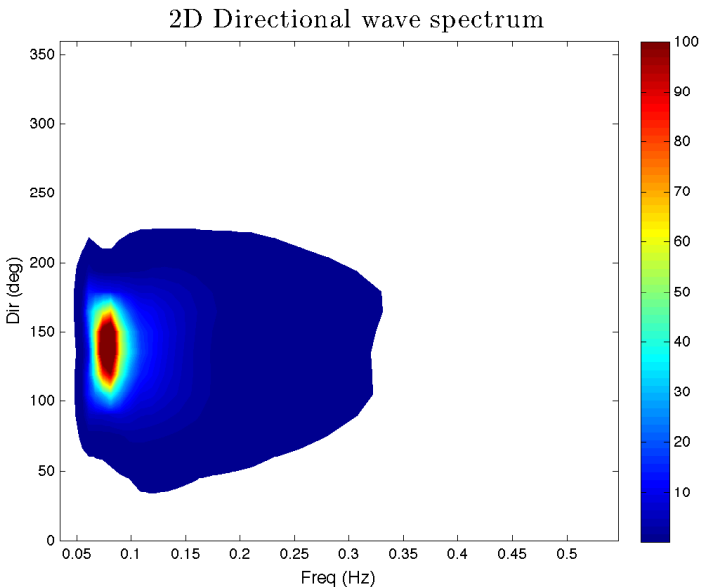


Figure: Directional spectrum  $E(\omega, \theta)$ , obtained from ECMWF

# Mathematical Framework

## Euler equations

Consider an inviscid, incompressible body of water whose motion is irrotational. The flow is then described by the velocity potential  $\phi(x, y, z, t)$  and dynamics of the flow are governed by the three dimensional Euler equations;

$$\nabla^2 \phi = 0, \quad \text{for } -\infty < z < \eta(x, y, t) \quad (2)$$

$$\phi_t + gz + \frac{1}{2} (\nabla \phi)^2 = 0, \quad \text{at } z = \eta(x, y, t) \quad (3)$$

$$\eta_t + \nabla_h \phi \cdot \nabla_h \eta = \phi_z, \quad \text{at } z = \eta(x, y, t) \quad (4)$$

where

- $\eta(x, y, t)$  is the free surface displacement
- $\nabla_h = (\partial/\partial x, \partial/\partial y)$  is the gradient operator in the x-y plane

On the free surface, the boundary conditions (3)-(4) can be rewritten as

$$\phi_t + gz + \frac{1}{2} (\nabla_h \psi)^2 - \frac{1}{2} W^2 \left\{ 1 + (\nabla_h \eta)^2 \right\} = 0, \quad (5)$$

$$\eta_t + \nabla_h \psi \cdot \nabla_h \eta - W \left\{ 1 + (\nabla_h \eta)^2 \right\} = 0, \quad (6)$$

where

- $\psi(x, y, t) = \phi(x, y, \eta(x, y, t), t)$
- $W = \frac{\partial \phi}{\partial z} \Big|_{z=\eta(x,y,t)}$



# Mathematical Framework

## HOSM

- The Higher Order Spectral Method (HOSM) was developed independently by Dommermuth & Yue and by West *et al.* in 1987.
- West *et al.*'s version has been found to be more consistent, and so their formulation is employed in this study.
- HOSM directly solves the Laplace equation for  $\phi$  at each time step by assuming a series expansion in the wave slope  $\varepsilon$  as solution.
- A series solution for  $W$  is then evaluated, which allows the time evolution of  $\eta$  and  $\phi$  to be followed via Eqns. (5)-(6)

Series expansion for  $\phi$ :

$$\phi(x, y, z, t) = \sum_{m=1}^M \phi^{(m)}(x, y, z, t) \quad (7)$$

where  $\phi^{(m)}$  is assumed to be of order  $O(\varepsilon^m)$ , and  $M$  is the order of nonlinearity

Taylor expanding each  $\phi^{(m)}$  around  $z = 0$  and collecting terms at each order;

$$\begin{aligned} \phi^{(1)}(x, y, 0, t) &= \psi(x, y, t), \\ \phi^{(m)}(x, y, 0, t) &= - \sum_{k=1}^{m-1} \frac{\eta^k}{k!} \frac{\partial^k}{\partial z^k} \phi^{(m-k)}(x, y, 0, t), \end{aligned} \quad (8)$$

Assuming the wave field is periodic in  $x$  and  $y$ ,  $\phi^{(m)}$  can be expressed as a Fourier series

$$\phi^{(m)}(x, y, z, t) = - \sum_k \sum_l a_{k,l}^{(m)}(t) e^{\kappa_{k,l} z} \exp\left(i \frac{2\pi k}{L_x} x\right) \exp\left(i \frac{2\pi l}{L_y} y\right)$$
$$\kappa_{k,l} = \left[ \left(\frac{2\pi k}{L_x}\right)^2 + \left(\frac{2\pi l}{L_y}\right)^2 \right]^{1/2} \quad (9)$$

Series expansion for  $W$ :

$$W(x, y, t) = \sum_{m=1}^M W^{(m)},$$
$$W^{(m)} = \sum_{k=0}^{m-1} \frac{\eta^k}{k!} \frac{\partial^k}{\partial z^k} \phi^{(m-k)}(x, y, 0, t), \quad (10)$$

All terms containing  $W$  in the boundary conditions (5)-(6) are handled in such a way that the consistency of ordering with respect to  $\varepsilon$  is retained

- Nonlinear interactions between free and bound wave modes are intrinsic to the Euler equations
- Thus, the HOSM is quite suited for looking at nonlinear generation mechanisms for rogue events (e.g. Benjamin Feir Instability)
- This includes quasi resonant interactions between modes, which global scale models can not process
- On the other hand, global scale models cover other important physical factors which the HOSM cannot, such as wind forcing

# Numerical Simulations

## Numerical Setup

Appropriate domains and runtimes must be chosen to ensure accurate simulations of the time evolution of the wave field

- Timescales are chosen in accordance with the Benjamin Feir timescale, to allow full development of modulational instabilities

$$T/T_p \sim O(\varepsilon^{-2}) \quad (11)$$

- Similarly, physical domain size is chosen so that

$$L_{x,y}k_p \sim O(\varepsilon^{-2}) \quad (12)$$

- With wave steepness taken as

$$\varepsilon = \frac{k_p H_s}{2} \quad (13)$$

A large number of Fourier nodes are needed;

- to acquire high resolution wave fields and refined statistics
- to ensure interpolation of coarse hindcast data does not shift the spectral peak

Thus

$$N_{x,y} = 1024$$

The order of nonlinearity is chosen so as to include nonlinear four wave interactions:

$$M = 4$$

# Numerical Simulations

## Input Data

Initial conditions for  $\eta$  and  $\psi$  were produced using the hindcast directional spectrum  $E(\omega, \theta)$  as follows:

- Interpolate  $E(\omega, \theta)$  over the higher resolution  $N_x \times N_y$  grid, and introduce random phase approximation

$$E(\omega, \theta) \rightarrow E(\omega, \theta) \exp(i\beta)$$

where  $\beta$  is a random variable uniformly distributed over  $[0, 2\pi]$

- Convert to wavenumber spectrum for  $\eta$ ,  $E(k_x, k_y)$ , via the deep water linear dispersion relation

$$\omega = \sqrt{gk} \tag{14}$$



- Note, this spectrum needs to be normalised, and its complex conjugate taken into account

$$\hat{\eta} = \frac{1}{2} \frac{g^{1/2}}{\|k\|^{3/2}} (E(k_x, k_y) + c.c.) \quad (15)$$

- $\hat{\psi}$  is easily obtained via linear wave theory.
- Finally, performing a two dimensional inverse FFT on both  $\hat{\eta}$  and  $\hat{\psi}$  yields the initial condition for  $\eta$  and  $\psi$

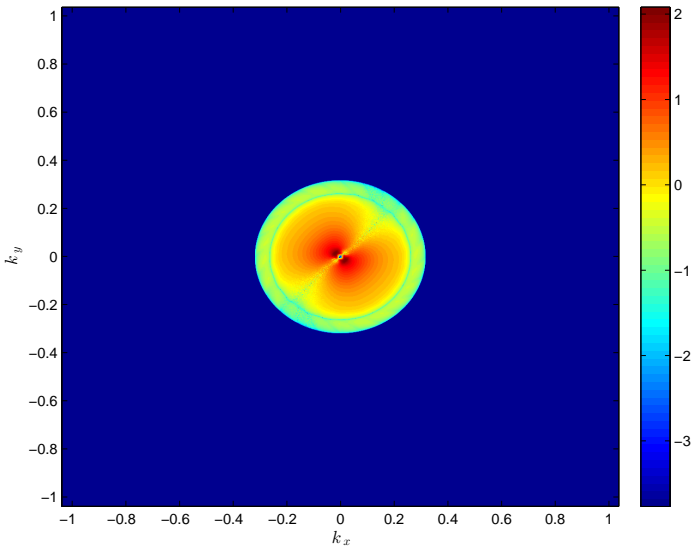


Figure: Wavenumber spectrum  $E(k_x, k_y)$  (log scaling)

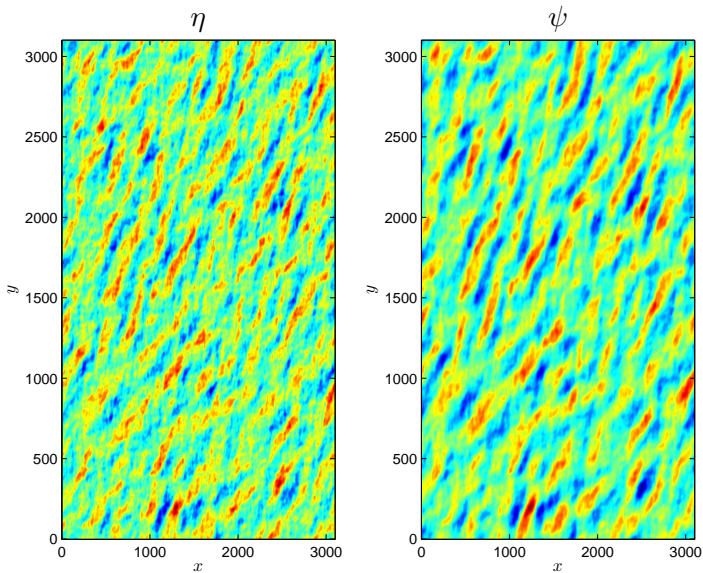


Figure: Initial Condition for  $\eta$  and  $\psi$

# Numerical Simulations

## Validity

Nonlinear interactions will be the primary generation mechanism considered. Most of the other mechanisms can be ruled out as candidates for the generation of the Andrea Wave:

- No strong currents were recorded during the Andrea event
- Wind-wave interactions occur over a much large time scale than that considered in this investigation
- The Andrea wave occurred in deep water, so shallow and bathymetry effects can be excluded
- We are investigating nonlinear wave fields, so linear focussing is not considered.
- No crossing sea state capable of influencing wave height statistics is present in the ECMWF hindcast data

# Preliminary Results

Some preliminary results from HOSM simulations of the Andrea wave field.

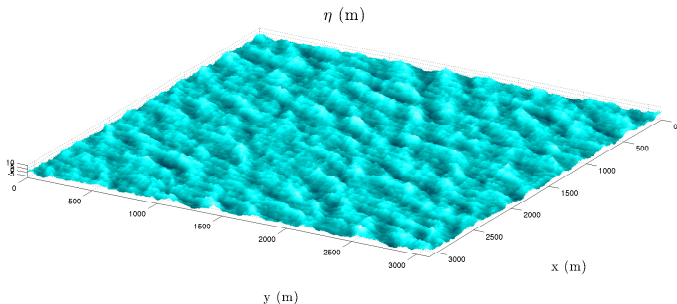


**Figure:** The free surface of the Andrea wave field, as simulated by HOSM

- The high resolution free surface output of the HOS allows for accurate measurement of important wave parameters. For example,  $\eta$ 's kurtosis is of particular importance in rogue wave science.
- It is well known that the behaviour of kurtosis is related to occurrence probability, with values above gaussian resulting in pdfs with higher tails corresponding to freak events.
- Also, kurtosis is again well known to correspond with the Benjamin Feir index, a measure of a wave's susceptibility to modulational instability.
- In the unidirectional limit, their relationship is linear. Such a limit does not apply to the Andrea wave field, and so kurtosis measurements are expected to be damped

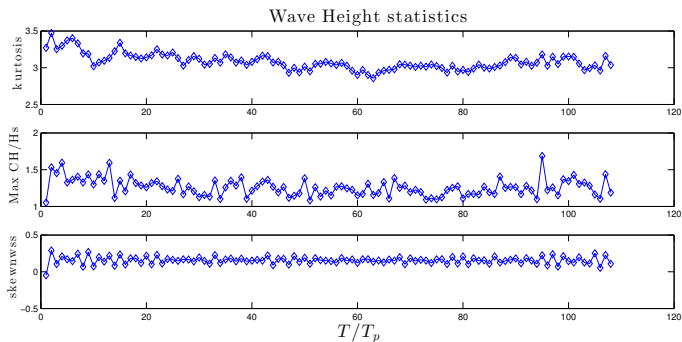


Figure: Time evolution of: kurtosis (top),  $CH_{max}/H_s$  (middle), skewness (bottom)

- Kurtosis measurements are shown to be above Gaussian, and correspondingly maximum values of the ratio  $CH_{max}/H_s$  are above rogue wave criteria.
- This implies that although the Andrea wave field is seen to be directionally spread, nonlinear effects are still important in the generation of freak events occurring within the field.
- Also non-Gaussian values of skewness are seen, again lending to freakish deviations from the normal Gaussian probability density function



# Conclusions

- Complimentary use of local scale phase resolved models (the HOSM) with global scale spectral models( Wavewatch III) can be highly beneficial
- Global scale models can provide realistic representations of sea states, and physical factors such as wind forcing that the HOSM can not process
- The HOSM can produce high resolution wave fields and refined wave statistics, as shown by this presentation
- Results are preliminary, although they are positive and encouraging. More simulations required for true statistical significance.

## Scope for future work:

- Investigate correlation between directional spread, spectral bandwidth, and kurtosis/BFI
- The influence of directional spread on the relationship between BFI and kurtosis
- Crossing sea states

# References I



E. M. BITNER-GREGERSEN, L. FERNANDEZ, J. M. LEFÈVRE, J. MONBALIU & A. TOFFOLI 2014;  
The North Sea Andrea storm and numerical simulations,  
*Natural Hazards and Earth System Sciences*, **14**, 1407-1415.



K DYSTHE, H. E. KROGSTAD, & P. MULLER 2008;  
Oceanic Rogue Waves, *Annual Review of Fluid Mechanics*






P. A. E. M. JANSSEN 2003;  
Nonlinear four-wave interactions and freak waves, *Journal of Physical Oceanography*, **33**, 863-884.



C. KHARIF & E. PELINOVSKY 2003;  
Physical Mechanisms of the Rogue Wave Phenomenon ,  
*European Journal of Mechanics B/Fluids*, 603-634.

# References II

-  [A. K. MAGNUSSON & M. A. DONELAN 2013;](#)  
The Andrea Wave - Characteristics of a Measured North Sea Rogue Wave, *Journal of Offshore Mechanics and Arctic Engineering*.
-  [N. MORI & P. A. E. M. JANSSEN 2006;](#)  
On Kurtosis and Occurrence Probability of Freak Waves, *Journal of Physical Oceanography*. **7**, 1471-1483.
-  [N. MORI, M. ONORATO & P. A. E. M. JANSSEN 2011;](#)  
On the Estimation of the Kurtosis in Directional Sea States for Freak Wave Forecasting, *Journal of Physical Oceanography*. **41**, 1484-1497.

# References III



M. TANAKA 2011;

A method of studying nonlinear random field of surface gravity waves by direct numerical simulation, *Fluid Dynamics Research*. **28**, 31-60.



B. J. WEST, K. BRUECKNER & R. S. JANDA 1987;

A New Numerical Method for Surface Hydrodynamics, *Journal of Geophysical Research*.



W. XIAO, Y. LIU, G. WU & D. K. P. YUE 2013;

Rogue Wave occurrence and dynamics by direct simulations of nonlinear wave-field evolution, *Journal of Fluid Mechanics*. **720**, 357-392.